Special Issue: DTD 2006 in JAPAN
Original Article
J. Jpn. Soc. Microgravity Appl. Vol. 24 No. 3 2007 (255-260)

The Effects of Gravity on Cryogenic Boiling Heat Transfer During The Tube Quenching at Low Mass Velocity

Teruo NISHIDA[1], Osamu KAWANAMI[1], Itsuro HONDA[1], Yousuke KAWASHIMA[1], Haruhiko OHTA[2]

[1] Department of Mechanical and System Engineering, University of Hyogo, 2167 Shosha, Himeji, Hyogo 671-2201, Japan, e-mail: kawanami@eng.u-hyogo.ac.jp
[2] Department of Aeronautics and Astronautics, Kyushu University, 744 Motooka, Nishi-ku, Fukuoka 819-0395, Japan

Abstract

We investigated the heat transfer during tube quenching for developing an on-orbit cryogenic fluid management system. This paper describes the experimental results of tube quenching for two flow directions (upflow and downflow) under terrestrial conditions. Liquid nitrogen (LN_2) is used as the test fluid, and it is injected into a transparent heated tube at a mass velocity of 100–600 kg/m^{2}s. The tube is made of pyrex glass, and it has an inner diameter of 13.6 mm and a wall thickness of 1.2 mm. The thermal data reveals that the quenching time during which the inner wall temperature became equal to the LN_2 boiling temperature (77.3 K) under upflow condition is less than that under downflow condition. The flow visualization data reveals the existence of a filamentary flow only under the downflow condition, and this flow pattern leads to a decrease in the cooling rate of the tube wall.

1. Introduction

During the re-ignition of a rocket engine in space, when a small amount of the residual propellant is transferred from the tank to the combustion chamber, it is important to precisely understand the difference between the phenomena that occur in space and those on the ground[(1)]. In addition, cryogenic propellants such as liquid hydrogen, liquid oxygen, and liquid helium require on-orbit management for future space transportation systems, such as on-orbit fluid resupply systems. On-orbit cryogenic fluid management is a technological aspect that will be common to all future space missions[(2, 3)].

Boiling under microgravity conditions has been investigated much earlier than adiabatic two-phase flows; these studies were initiated during the early 1960s, and they continue till today. However, most studies on microgravity boiling focused particularly on pool boiling. On the other hand, flow boiling (different from pool boiling and adiabatic two-phase flow) has not been thoroughly investigated in the past. In particular, very few experiments on cryogenic flow boiling under microgravity conditions have been conducted; this can be attributed to the fact that these experiments are by far the most difficult and complex boiling experiments.

Antar *et al.*[(4)] reported the flow visualization and measurements for the flow boiling of liquid nitrogen (LN_2) in tubes aboard a KC-135 aircraft. They identified a new vapor/liquid flow pattern that is unique under microgravity conditions. This pattern is composed of a long and connected liquid column flowing in the center of the tube and surrounded by a thick vapor layer. The vapor annulus that separates the liquid filament from the wall is considerably thicker than that observed in the terrestrial experiment. With regard to heat transfer, it was reported that under microgravity conditions, the quenching process was delayed and the cooling rate of the tube wall decreased. However, these experiments did not report the heat transfer characteristics of the quenching process, such as the heat flux and heat transfer coefficient. In addition, the terrestrial and microgravity experiments were generally not conducted under similar mass velocity conditions.

To clarify the effects of gravity on heat transfer during quenching of the propellant transfer line, we investigated the cryogenic forced convective boiling. Thus far, we have reported that, under microgravity conditions, the quenching time is approximately 1.2 times shorter and the maximum and minimum heat fluxes are approximately 1.4 and 1.2 times greater than those under terrestrial conditions, respectively[(5)].

In general, conducting repeated microgravity experiments using drop towers and aircrafts is extremely expensive. Therefore, experiments to investigate the effects of gravity on cryogenic boiling heat transfer need to be conducted under terrestrial conditions.

Earlier, Zhang *et al.*[(6)] investigated the effects of orientation on the flow boiling critical heat flux (CHF) under saturated and subcooled conditions for the normal fluid. Experiments were performed using a coolant along the vertical and inclined upflow and downflow directions, as well as the horizontal flow direction, and with the heated surface directed upward or downward with respect to gravity. They reported that the CHF value was extremely sensitive to orientation for a flow velocity below 0.2 m/s and the saturated flow condition. The effects of orientation weaken considerably for velocities greater than 0.5 m/s for both the saturated and subcooled flow.

The present study aims to understand the effects of gravity on cryogenic boiling heat transfer during tube quenching. Here, we report the

experimental results of cryogenic forced convective boiling for two flow directions (upflow and downflow) under terrestrial conditions.

2. Experimental Apparatus and Procedure

2.1 Experimental apparatus

A schematic diagram of the experimental apparatus used in this study is shown in **Fig. 1**, and a detailed drawing of the test section is shown in Fig. 2. The apparatus mainly consists of the test section, LN_2 and gaseous nitrogen (GN_2) tanks, vacuum pump (ULVAC, DA-15D), data logger (KEITHLEY, 2701), level meter (AMERICAN MAGNETICS, INC., MODEL 185), and CCD camera (TOSHIBA Co., IK-CU44). For safety considerations, LN_2 is selected as the test fluid in the present experiments; in addition, LN_2 is a suitable model for liquid oxygen and liquid hydrogen.

2.2 Transparent heated tube

The test section consists of a transparent heated tube[7, 8], which is surrounded by vacuum insulation and is vertically oriented under terrestrial conditions. The tube is made of pyrex glass, and it has an inner diameter (ID) of 13.6 mm and an outer diameter (OD) of 16 mm. The temperature measurement length is approximately 150 mm, and its inner wall is uniformly coated with a transparent gold film with a thickness of 0.01 μm. The film is used as a resistance thermometer to directly evaluate the inner wall temperature averaged over the entire temperature measurement length. Additionally, the transparency of the film allows a visual observation of the flow behavior through the wall. Both ends of the tube are coated with a thick layer of silver film for use as electrodes and are in contact with a duralumin flange, as shown in the right side of **Fig. 2**.

The arrow in this figure that indicates the flow direction is fixed for the test section. The downflow experiment is conducted by rotating the test section by 180 degrees.

To measure the temperature distribution along the flow direction, this measurement region was divided into three 50-mm-long segments. **Figure 3** shows the relationship between the temperature and resistance of the thin-gold-film-coated inner wall of the tube in the cryogenic temperature region. As shown in this figure, the temperature of the inner wall of the tube was found to be proportional to the resistance of the thin gold film within the three segments. As an example of tube quenching, we could obtain the temperature histories for the three segments, as shown in **Fig. 4**. The starting of the

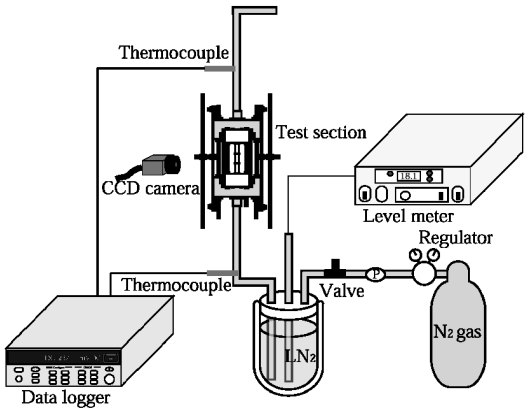

Fig.1 Schematic diagram of the experimental apparatus.

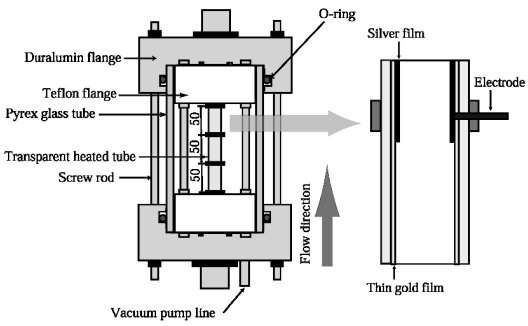

Fig.2 Detailed view of the test section with transparent heated tube.

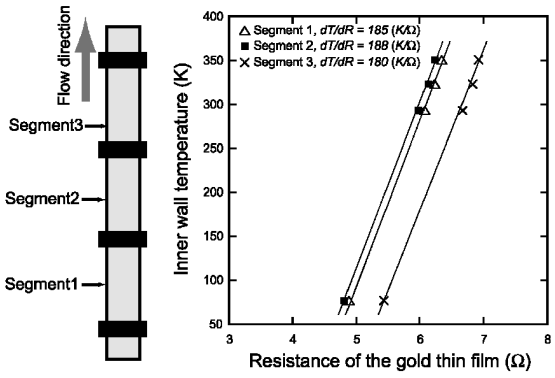

Fig.3 Relationship between the inner wall temperature and resistance of the thin gold film coated on the inner wall of the tube in the cryogenic temperature region.

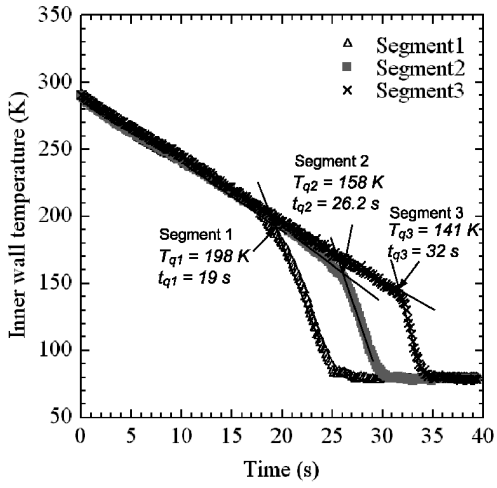

Fig.4 Example of the temperature histories for the three segments (G = 98 kg/m^{2}s, upflow).

liquid nitrogen flowing is set to 0 second in this paper.

2.3 Mass velocity measurement

In the present study, the mass velocity G is measured by using the level meter installed in the supply tank; G can be determined by measuring the displacement of the LN_2 surface in the supply tank. The value of G is controlled by GN_2 pressure injected into the supply tank. **Figure 5**(a) shows the histories for three different values of G (98, 297, and 506 kg/m^{2}s). At the beginning of tube quenching, the value of G is unstable; therefore, we define it as the averaged value from the quench point at segment1 (indicated by arrows in Fig. 5(a)) to the end of the experiment that is complete quenching of tube. Figure 5(b) shows the value of G versus GN_2 pressure based on these measurement methods. The error bar in Fig. 5(b) is defined as the width of mass velocity between the time pointed by arrow and the time of complete tube quenching for each experiment.

2.4 Experimental procedure

The experiments were conducted for G = 100–600 kg/m^{2}s. Initially, GN_2, whose pressure is controlled by a pressure regulator, expels LN_2 from its tank toward the test section. The initial temperature of the test section is maintained at room temperature (approximately 300 K). The flow behavior in the tube is observed with a CCD camera, and the temperature of the inner wall of the tube is measured by using a gold film as a resistance temperature sensor. The output of the test section is released into the atmosphere.

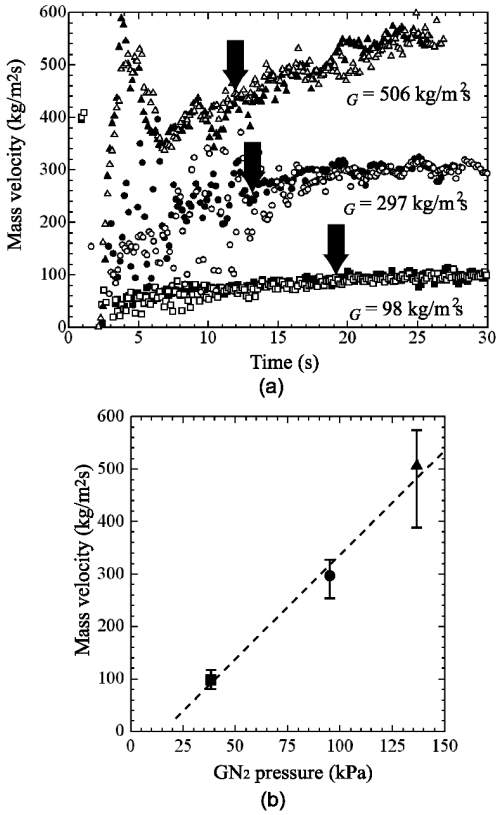

Fig.5 (a) LN_2 mass velocity measured using the level meter. (b) The value of G versus GN_2 pressure (■: G = 98 kg/m^{2}s, upflow; ●: G = 297 kg/m^{2}s, upflow; ▲: G = 506 kg/m^{2}s, upflow; □: G = 100 kg/m^{2}s, downflow; ○: G = 292 kg/m^{2}s, downflow; △: G = 509 kg/m^{2}s, downflow).

3. Results and Discussion

3.1 Thermal characteristics

The quenching process is divided into three distinct heat transport regions, which are appropriate to describe the quenching problem. The first region comprising the temperature segment beginning at the initial tube wall temperature and terminating at the point of shape drop in temperature is termed the film boiling region. The next region comprising the maximum temperature drop, which occurs after the quench front temperature is attained, is termed the nucleate boiling region. Finally, the segment with no significant temperature drop is termed the forced convection region. These three different flow regions are shown in **Fig. 6**. It should be noted that

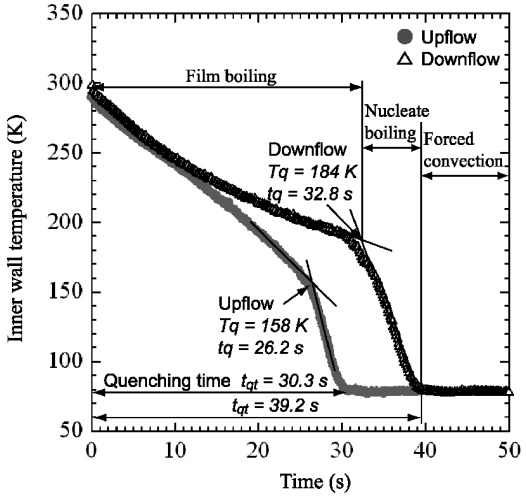

Fig.6 Inner wall temperature histories for G = 100 kg/m^{2}s (at segment2).

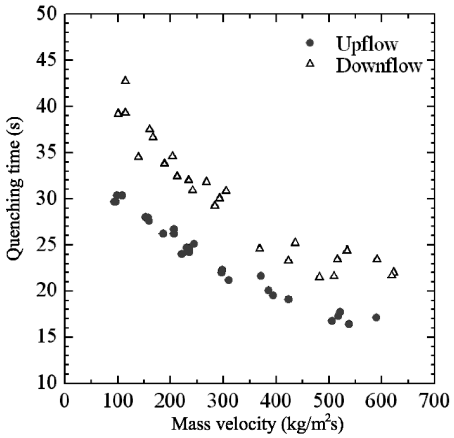

Fig.7 Variations in t_{qt} with G (at segment2).

the transition from the film boiling region to the nucleate boiling region is distinctly characterized by different slopes of the temperature history curves. The slope for the nucleate boiling region is considerably steeper than that of the film boiling region. The main reason for the different cooling rates is that the wall is totally covered by vapor in the film boiling region, which results in very low heat transfer rates. In the nucleate boiling region, portions of the wall experience direct contact with the liquid, which drastically increases the heat transfer.

In this study, the definition of the quench front temperature is similar to the apparent rewetting temperature described by Barnea *et al*[9]. The quench front temperature T_q is defined as the intersection point between the line tangent to the temperature-time curve at the location with the largest slope and the line tangent to the curve before quenching.

Figure 6 shows a comparison between the inner wall temperature histories for the upflow and downflow conditions for G = 100 kg/m^{2}s. This figure clearly shows that when LN_2 comes in contact with the inner wall of the tube under the downflow condition, the value of T_q is greater than that under the upflow condition. The quenching time t_{qt} during which the inner wall temperature became equal to the LN_2 boiling temperature (77.3 K) under the upflow condition was less than that under the downflow condition. In **Fig.7**, maximum and minimum heat fluxes are plotted for G = 100–600 kg/m^{2}s.

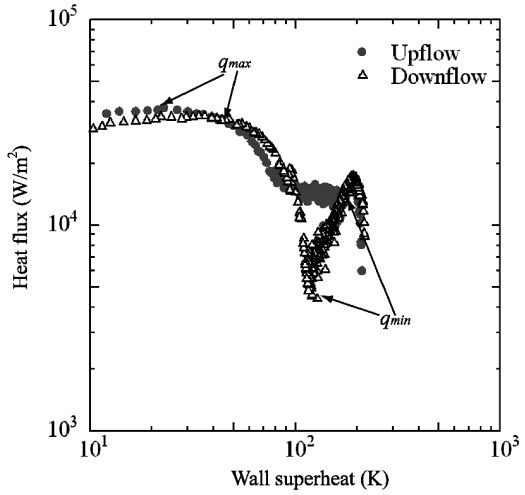

Fig.8 Boiling curve for G = 100 kg/m^{2}s (at segment2).

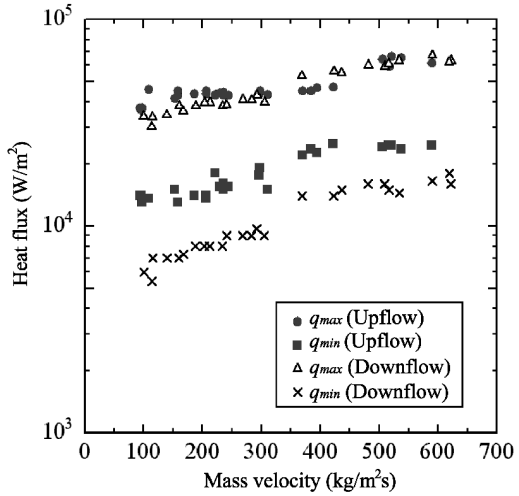

Fig.9 Variations in q_{max} and q_{min} with G (at segment2).

Next, we consider the heat transfer characteristics, such as the heat flux. **Figure 8** shows the boiling curve for G = 100 kg/m^{2}s. The minimum heat flux q_{min} under the downflow condition is smaller than that under the upflow condition. The maximum heat flux q_{max} is almost similar under the upflow and downflow conditions. In **Fig. 9**, q_{min} and q_{max} are plotted for G = 100–600 kg/m^{2}s. Usually, the gravity effects on heat transfer of forced convective boiling decrease with an increase in the mass velocity. In this study however unique phenomena were found on the heat transfer; the difference on t_{qt} and q_{min} between upflow and downflow did not decrease with an increase in the mass velocity.

On the basis of these results, it was found that the heat flux in the film boiling region influences the value of t_{qt}; the heat flux in the film boiling region under the downflow condition is smaller than that under the upflow condition, which increases the value of t_{qt} under the downflow condition.

3.2 Flow visualization

The photographs in **Fig.10** and **Fig.12(a)** show the flow behavior observed during tube quenching under the upflow and downflow conditions for G = 105 kg/m^{2}s. The droplet size under the upflow condition was greater than that under the downflow condition. In addition, it was found that before quenching, the flow under the upflow condition was more disturbed than that under the downflow condition. These two differences under the upflow and downflow conditions were related with the results evident from Fig. 6 and Fig. 9: the large droplets and disturbed flow under upflow conditions enhanced the heat transfer during tube quenching, resulting in a decrease in the value of t_{qt} and increase in the heat flux.

The photographs in **Fig. 11** and **Fig. 12(b)** show the flow behavior observed during tube quenching under the upflow and downflow conditions for G = 590 kg/m^{2}s. A filamentary flow (as reported by Antar *et al.*[4]) was observed as shown in the circle in Fig. 11(b). This flow pattern comprised a long and connected liquid column surrounded by a thick vapor layer and flowing in the center of the tube. The vapor layer, which separated the liquid from the wall of the tube, is considerably thicker than that occurring in the inverted annular flow pattern. In the

present experiment, this filamentary flow was observed under the conditions of downflow and over G = 350 kg/m^{2}s. Furthermore, this flow pattern was not observed under the upflow conditions. The velocity difference between vapor and liquid is suppressed in downward flow and high mass velocity conditions. Therefore, the filamentary flow is created in these conditions. The influence by the difference of flow pattern clearly appeared to the change in the minimum heat flux in Fig. 7 and Fig. 9.

4. Conclusions

This study investigated the effects of gravity on heat transfer during quenching of the fuel transfer line under terrestrial conditions. A transparent heated tube was employed for observing the fluid behavior and measuring the heat transfer during tube quenching under the upflow and downflow conditions. LN_2 is used as the test fluid, and it is injected into the transparent heated tube for G = 100–600 kg/m^{2}s.

For mass velocities below 350 kg/m^{2}s, a large droplet size and disturbed flow enhanced the heat transfer during tube quenching, resulting in a decrease in the value of t_{qt} and increase in the heat flux.

For mass velocities greater than 350 kg/m^{2}s, a filamentary flow was observed. Furthermore, the filamentary flow pattern was not observed under the upflow condition. Further, the results indicate that the filamentary flow pattern leads to a decrease in the cooling rate of the tube wall.

Acknowledgement

A part of this study was supported by a research grant from the Matsuda Foundation.

References

1) A. Pacros, J. Follet and B. Vieille: *Proc. Microgravity Transport Processes in Fluid, Thermal, Biological and Materials Science Conf. III*, Davos, Switzerland, ECI: MTP-03-34. Sept. 2003.
2) T. Tanabe and S. Nakasuka, Preprints of 43rd Congress of IAF, IAF-92-0168, 1992.
3) L. J Hastings *et al.*, *AIAA/NASA/OAI Conference on Advanced SEI Technologies*, No. 91-3474, 1991.
4) B. N. Antar and F. G. Collins, *Int. J. Microgravity Research and Appl., X/3*, 118, 1997.
5) O. Kawanami *et al.*: *Proc. The 6th ASME/JSME Thermal Eng. Joint Conf.*, TED-AJ03-361 2003.
6) H. Zhang, I. Mudawar and M. Hasan, *Int. J. Heat Mass Transfer*, **45**, 4079–4095, 2002.
7) H. Ohta *et al.*, *ASME/JSME Thermal Eng. Conf.* **4**, 547–554, 1995.
8) H. Ohta, Microgravity heat transfer in flow boiling, Advances in Heat Transfer 37, Academic Press, 2003, pp. 1–74.
9) Y. Barnea, E. Elias, *Int. J. Heat Mass Transfer*, **37**, 1441–1453, 1994.

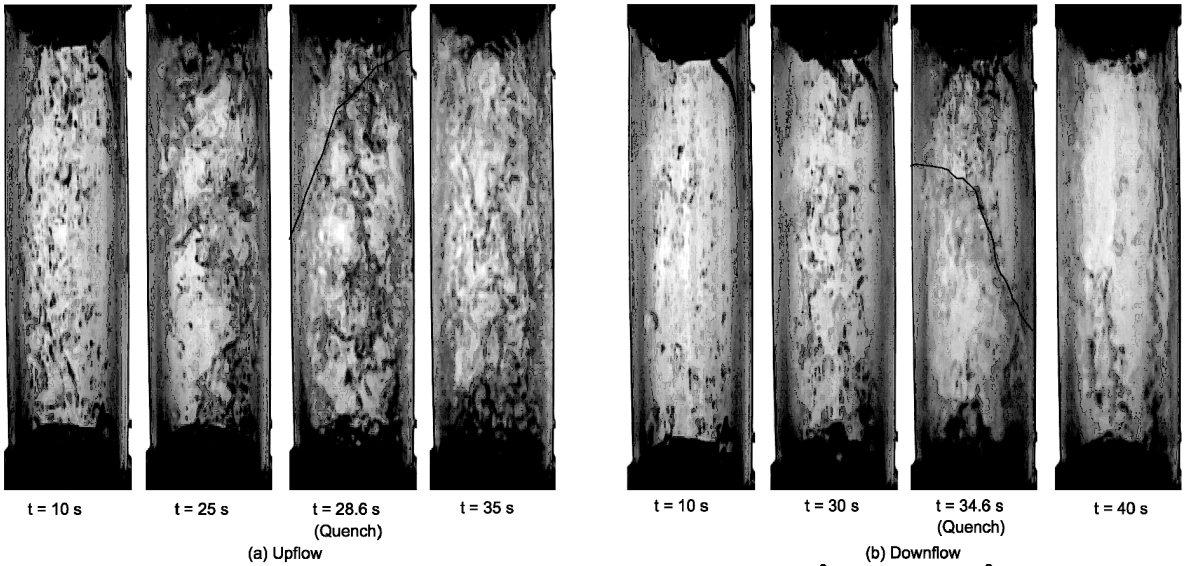

Fig. 10 Four single frames during tube quenching for values of G below 350 kg/m^{2}s (G = 105 kg/m^{2}s, at segment2). The quench front line was observed at (a) t = 28.6 s and (b) t = 34.6 s.

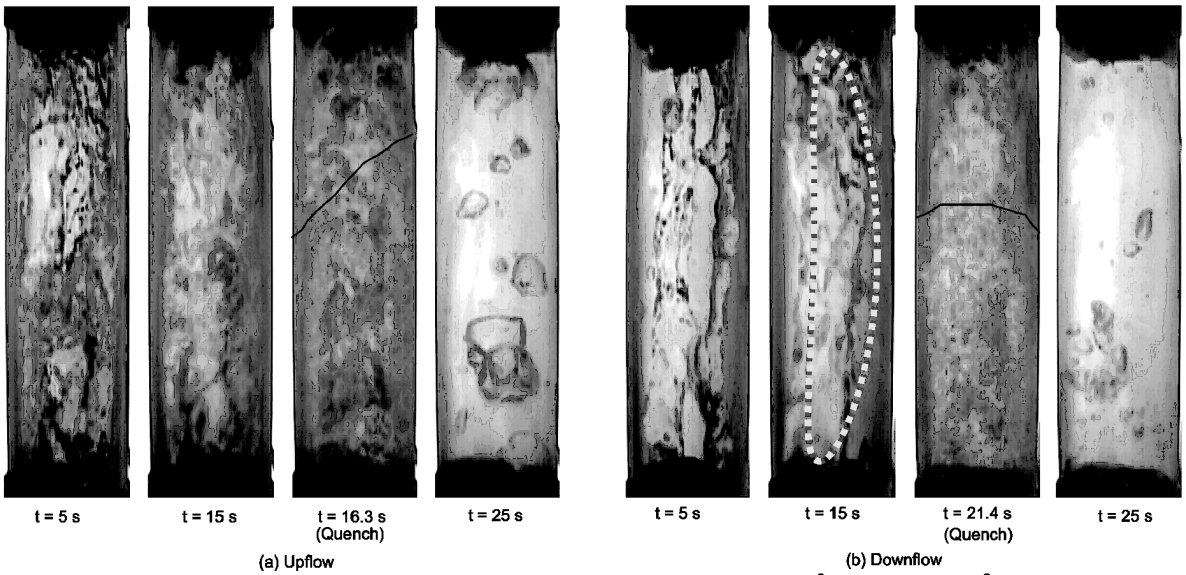

Fig. 11 Four single frames during tube quenching for values of G above 350 kg/m^{2}s (G = 590 kg/m^{2}s, at segment2). The quench front line was observed at (a) t = 16.3 s and (b) t = 21.4 s.

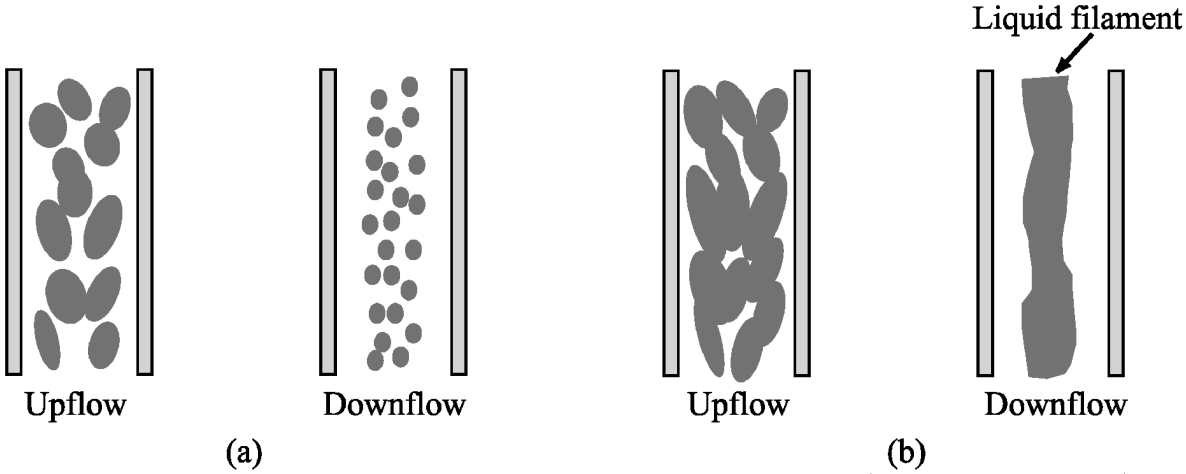

Fig. 12 Schematic diagrams during tube quenching for values of G (a) below 350 kg/m^{2}s and (b) above 350 kg/m^{2}s.

Received October 23, 2006
Accepted for publication, July 14, 2007